

Design of Low-Index Metamaterial Lens Used for Wideband Circular Polarization Antenna

Yong Wang and Yanlin Zou*

Abstract—A novel low-index metamaterial lens (LIML) used for wideband circular polarization antenna is proposed. With gradual spaces between metamaterial elements of the LIML, a much wider bandwidth can be achieved than that of the LIML with equal element space. A planar equiangular spiral antenna with reflector is used to demonstrate the design idea of the proposed LIML. By using the specially designed LIML, the ultimate antenna can achieve an obvious gain improvement of 2 dBi and a wide axial ratio bandwidth of 44% (from 6.9 GHz to 10.8 GHz). A prototype is fabricated, and the measured results agree well with the simulated ones.

1. INTRODUCTION

Owing to the huge development of wireless technology, applications like wide-band point-to-point communication system are highly demanded in people's routine life. However, antenna design for such a system is quite a challenge because of the tough requirements such as wide operating band, circular polarization (CP) and high gain. Additionally, compact size is also preferred to ensure the mobility of the device. A planar antenna is well known for its features of low profile, compact size and easy fabrication, which make it a common choice for these applications. However, low gain of the antenna element is a drawback which limits the system performance. Conventional way of gain enhancement is to use several antenna elements to construct an antenna array, but it needs complex feed system and will cause extra loss. Moreover, the much larger volume of antenna array is usually not accepted.

In recent years, many research groups have realized low/zero-index metamaterial (LIM/ZIM) through experiments [1–3]. According to Snell's law, when the ray is incident from inside the LIM/ZIM into free space, the angle of refraction will be close to zero, so the refracted rays will be normal to the interface [3]. This feature provides an effective method for gain enhancement. Essentially, it is a resonant structure which can improve the gain of specified antenna in some frequency band. However, most of the published LIM or ZIM structures can only be applied to linearly polarized antenna and act in narrow bandwidth. In [4], to broaden the frequency band of ZIML adaptive for the linearly polarized antenna, a Z-shaped element has been proposed. By combining the electric and magnetic constitutive elements in a volumetric metamaterial unit cell, the collimating lens in [5] produces directive radiation with dual linear polarizations, and potentially, with circular polarizations, yet the structure of its metamaterial slab is rather complex and its performance in CP antenna is untestified. To realize an unidirectional pattern and keep the CP characteristic of spiral antenna in a wide frequency band, a metamaterial absorber is designed in [6], but the antenna gain is relatively low since the backward radiation has been absorbed. As we all know, many of the wideband antennas, such as spiral antennas and log-periodic antennas, have gradual structures so that different parts are corresponding to different resonant frequencies. So we hope to verify whether this type of structure can be used to expand the bandwidth of LIML.

Received 20 March 2017, Accepted 27 May 2017, Scheduled 9 June 2017

* Corresponding author: Yanlin Zou (ylzou@mail.xidian.edu.cn).

The authors are with the Science and Technology on Antenna and Microwave Laboratory, Xidian University, Xi'an, Shaanxi 710071, China.

In this letter, we present a LIML which can improve the gain of wideband circular polarization antenna. A metamaterial structure competent for circular polarization is used as the element to design the LIML adaptive for wideband and circular polarization antenna. A planar equiangular spiral antenna, with a metal plate as reflector to realize unidirectional radiation, is selected as the object to expand our design process of LIML. To verify our design, a comparative experiment is carried out and will be presented in the later sections.

2. DESIGN AND THEORY

2.1. LIML Unit Cell

A metamaterial unit cell in Fig. 1 is used as basic element to create the proposed metamaterial lens. This unit cell is a type of special resonant structure, and its dimensions are optimized delicately to ensure that the metamaterial lens can enhance the antenna gain without deteriorating the circular polarization performance. The unit cell consists of a metallic patch and an FR-4 substrate with thickness of 1 mm and relative permittivity $\epsilon_r = 4.4$. Fig. 1 shows the model in simulation software. Due to the periodicity, one unit cell with master and slave boundary conditions on the side faces is sufficient to simulate the characteristic parameters of entire metamaterial array.

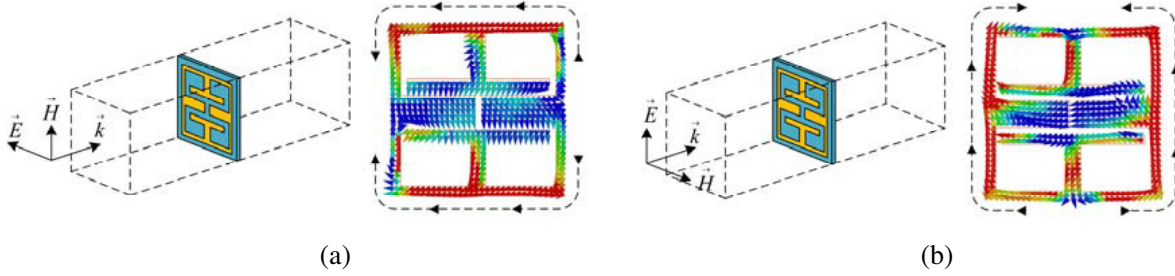


Figure 1. Geometry and current distribution of the simulated LIML unit cell: (a) Horizontal excitation and (b) vertical excitation, master and slave boundary conditions are configured on the side faces.

It is known that one of the basic requirements for achieving circular polarization is that the magnitudes of the two orthogonal field components are similar. So, when a plane wave passes through LIML, the magnitudes of the two orthogonal field components should keep the same. Here are some definitions: when the E component of plane wave is parallel with the metal strips in the center of the unit cell, it is called horizontal excitation (HE, Fig. 1(a)); when the E component of plane wave is vertical to these strips, it is called vertical excitation (VE, Fig. 1(b)). Fig. 1(a) and Fig. 1(b) show the current distribution when the unit cell is illuminated by HE and VE, respectively. It can be observed that strong surface current (dashed line with arrows) flows through the upper and lower edges of the metal patch when HE is imposed, whereas the strong surface current appears on the left and right edges of the metal patch if VE is imposed. Just as depicted in Fig. 1, by delicately adjusting the structure of this unit cell, the magnitudes of excited current under the two above mentioned excitations are almost identical, and then the CP characteristic of LIML is realized.

2.2. Wide-Band Metamaterial Slab and Antenna Configuration

Referencing the broadband mechanism of the planar equiangular spiral antenna, we suppose that, to improve the performance of this antenna in a wide band, the metamaterial unit cells should obey a similar rule. That is, their sizes and spaces should also be gradual from the center to the outside. In our simulation, it is found that the gradual cell sizes contribute no obvious positive effect on the antenna performance. Hence, in the subsequent design process, all the unit cells are kept the same in shape and size, and only the spaces between them are considered as the optimization parameters.

The optimization goal is that, by using the LIML, the original antenna will have an obvious improvement on the gain and bandwidth, especially the axial ratio (AR) bandwidth. This procedure is

carried out by using trial and error in EM simulation software HFSS16.0. The optimized spaces between LIML cells and other detailed structures are shown in Fig. 2(a). The total height is 26.4 mm, which is only 0.6 times of the wavelength of the lowest frequency. The spiral antenna is composed of two printed radiation patches and backed with a metal reflector. The whole system is fed by a coax taper balun on the bottom.

Since the extraction of equivalent refraction index of gradual structures is much more difficult, as an alternative measure, we just extract the equivalent refraction indexes of several different equal-space structures to illustrate their variations with frequency. The extraction algorithm presented in [8] is employed and the calculated refraction index curves are shown in Fig. 2(b). Note that DX indicates the distance between adjacent elements in the equal-space LIML. As it can be seen from Fig. 2(b), for these four distances, it has some frequency ranges in which $|n| < 1$ is satisfied. According to Snell's law, a lens with low index, typically when $|n| < 1$, has the ability to achieve gain enhancement. Moreover, as shown in Fig. 2(b), with the element spaces becoming wider, the range $|n| < 1$ shifts to lower ends of the frequency band. It implies a trend that the gain enhancement ability of the equal-space LIML shifts to lower frequency when the element space becomes larger. Therefore, when we introduce the gradual spaces between metamaterial elements and make their locations corresponding to the gradual radiation parts of antenna, the antenna gain can be improved in a wide frequency range.

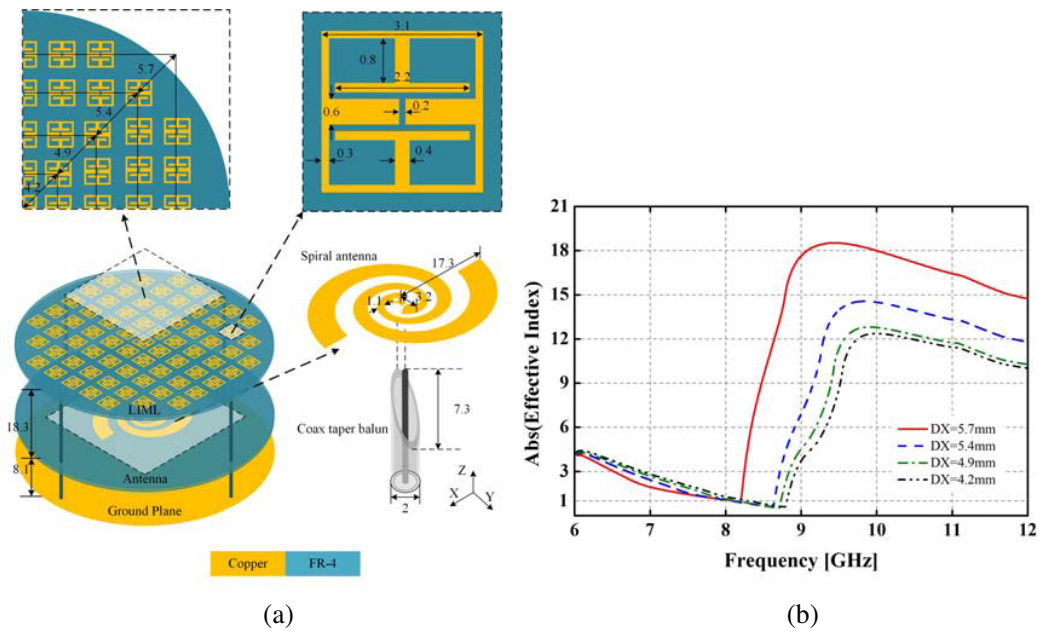


Figure 2. (a) Structures of spiral antenna with proposed LIML (Unit: mm). (b) Effective material index for different unit cell spaces.

3. SIMULATED AND MEASURED RESULTS

3.1. Performance Comparison

A prototype of spiral antenna with optimized LIML is fabricated to validate our idea, which is shown in Fig. 3. The input impedance measurement is performed by using Agilent vector network analyzer E8363B. The measured and simulated results have the same trend, but there are some little differences between them. This may be attributed to the fabrication precision of the antenna and the loss of coaxial cable.

For the simplicity of descriptions, the conventional LIML with equally-spaced elements is denoted as CLIML, and our presented LIML with nonuniform element spaces, which can be adaptive for the wideband circular polarization antenna, is denoted as WLIML. In order to evaluate the performance of

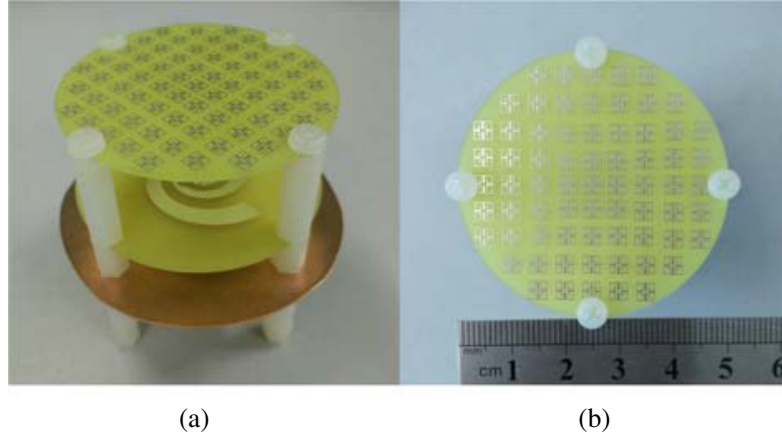


Figure 3. Prototype of spiral antenna with optimized LIML: (a) perspective view, (b) top view.

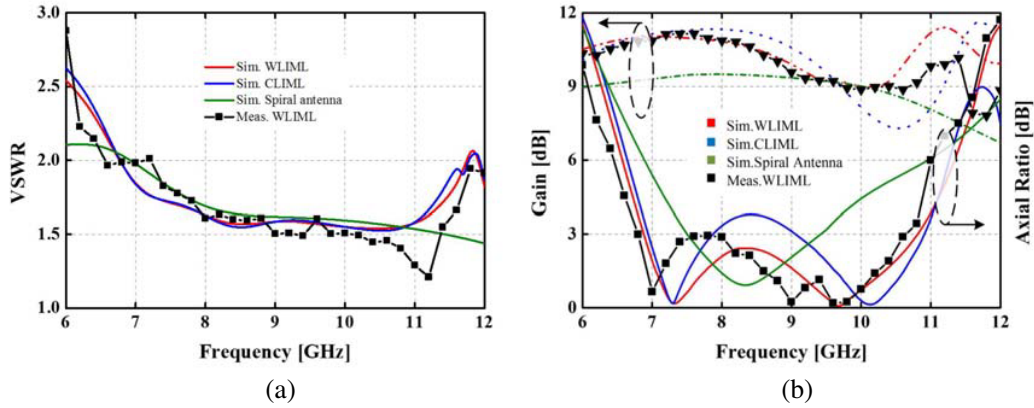


Figure 4. Comparisons between different configurations: (a) VSWR, (b) gain and AR.

the proposed metamaterial lens, comparisons that include VSWR, axial ratio (AR) and gain are made between the following three configurations, they are (1) spiral antenna with reflector, (2) spiral antenna with reflector and CLIML, (3) spiral antenna with reflector and WLIML.

The simulated VSWR curves of all the three configurations are demonstrated in Fig. 4(a), and only a small shift is observed in the higher frequency band when the antenna is configured with CLIML and WLIML, respectively. The measured VSWR curve has a similar tendency with the simulated one, which is lower than 2 from 6.6 GHz to 12 GHz and has a wide impedance bandwidth of at least 60%. So, it can be concluded that the addition of LIML does not deteriorate the impedance bandwidth obviously.

Next, the AR performance is compared and shown in Fig. 4(b). Influenced by the PEC reflector, the AR bandwidth of the spiral antenna with reflector is much narrower (only 21.3%) than that when it is located in free space. We can see that the AR of antenna with CLIML is higher than 3 dB in center region of the frequency band (7.8 GHz–9.1 GHz). For antenna with WLIML, an obvious improvement on AR bandwidth, up to 44% (from 6.9 GHz to 10.8 GHz), is achieved.

Figure 4(b) also shows the gain at boresight direction (+z axis) over the frequency band. The spiral antenna with reflector has an average gain of 9.0 dB in the most part of the working band. When CLIML is configured above the spiral antenna, an obvious gain enhancement is obtained from 6 GHz to 10 GHz. Compared with CLIML, the gain of WLIML is slightly lower in 6.9 GHz–9.7 GHz but higher in 9.7 GHz–11.4 GHz, so the LIML with gradual space provides a more stable gain improvement over the entire working band. However, it is also found that the gain falls at around 10 GHz when LIML is configured. According to the theory in [7], the resonance distance l of the presented LIML can be

determined by the following relation:

$$l = \left(\frac{\varphi_0}{360^\circ} - 0.5 \right) \frac{\lambda}{2} + N \frac{\lambda}{2}, \quad N = 0, 1, 2, 3, \text{ ect.}$$

where φ_0 is the phase of the reflection coefficient. The ideal height l for the maximum gain enhancement, with $\varphi_0 \approx 180^\circ$ and $N = 1$, is 0.5λ . As for our configuration, the actual height of WLIML is 18.7 mm, which meets the resonance condition and the maximum gain is obtained at around 8.2 GHz (18.7 mm is equal to 0.5λ of 8.2 GHz). When frequency gets higher, the above condition is no longer satisfied and it causes the gain degradation at around 10 GHz.

3.2. Radiation Patterns

As is shown in Fig. 5, the simulated and measured radiation patterns of the antenna with optimized WLIML are taken at 7 GHz, 8.5 GHz and 10.5 GHz, and stable radiation pattern is achieved in the whole frequency band. The antenna radiation pattern is almost invariably symmetrical along the z axis and the peak gain of co-polarization is higher than 8.5 dB. It can be seen that, by the loaded WLIML, the radiation beam is well focused, with sufficiently low side lobes and cross-polarization level.

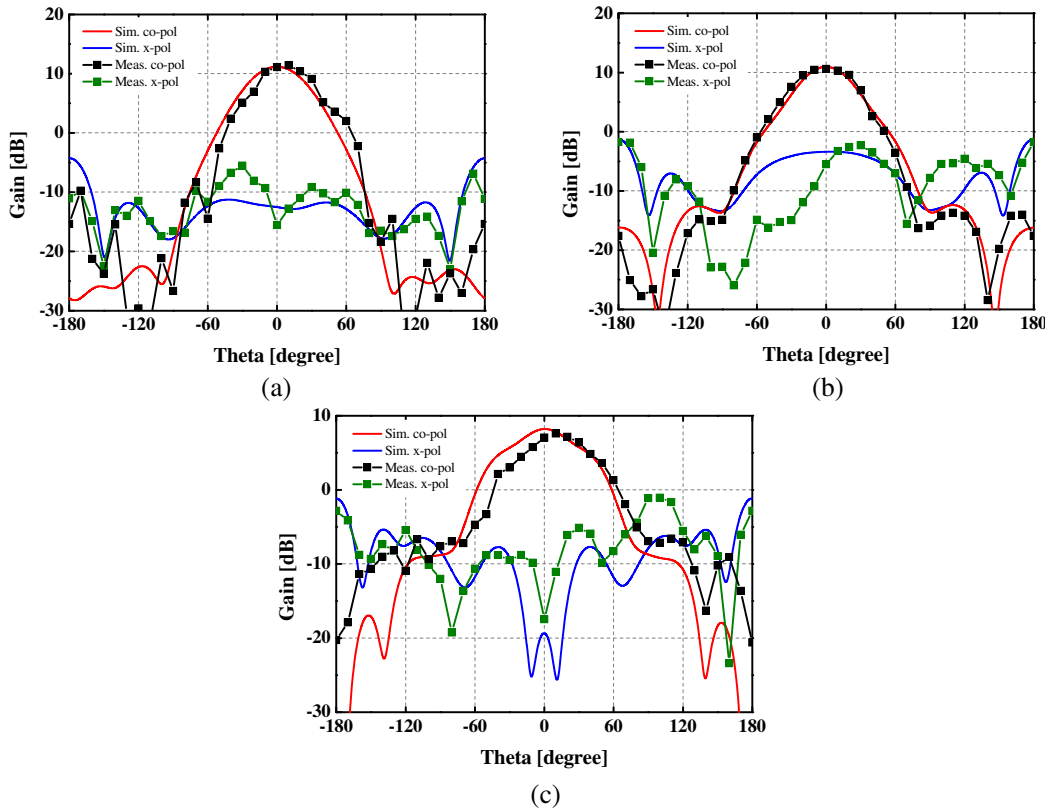


Figure 5. Measured and simulated radiation pattern at (a) 7 GHz, (b) 8.5 GHz and (c) 10.5 GHz.

4. CONCLUSION

By optimizing the dimensions of LIML element and the spaces between them, the function of LIML is extended and can be used to improve the gain while still preserves the AR bandwidth of wideband circular polarization antenna. A planar equiangular spiral antenna with reflector is selected as the object to expand our design process of LIML. Both simulated and measured results validate the effectivity of our design. The design idea of the proposed LIML can also be extended to the design of many other types of wide band CP antennas.

REFERENCES

1. Turpin, J. P., Q. Wu, D. H. Werner, B. Martin, M. Bray, and E. Lier, "Near-zero-index metamaterial lens combined with AMC metasurface for high-directivity low-profile antennas," *IEEE Trans. Antennas Propag.*, Vol. 62, 1928–1936, 2014.
2. Augustin, G., B. P. Chacko, and T. A. Denidni, "A zero-index metamaterial unit-cell for antenna gain enhancement," *IEEE International Symposium on Antennas and Propagation & USNC/URSI National Radio Science Meeting*, 126–127, July 2013.
3. Zhou, H., Z. Pei, S. Qu, S. Zhang, J. Wang, Z. Duan, H. Ma, and Z. Xu, "A novel high-directivity microstrip patch antenna based on zero-index metamaterial," *IEEE Antennas and Wireless Propag. Lett.*, Vol. 8, 538–541, 2009.
4. Lv, Y., F. Meng, J. Hua, and M. Chen, "A wideband zero index metamaterial lens for directive emission based on z-shaped meta-atom," *5th Global Symposium on Millimeter Waves (GSMM)*, 418–421, May 2012.
5. Turpin, J. P., Q. Wu, D. H. Werner, B. Martin, M. Bray, and E. Lier, "Low cost and broadband dual-polarization metamaterial lens for directivity enhancement," *IEEE Trans. Antennas Propag.*, Vol. 60, 5717–5726, 2012.
6. Louertain, K. and T. H. Chio, "Low-profile broadband spiral antenna with meta-materials," *IEEE Antennas and Propagation Society International Symposium (APSURSI)*, 1331–1332, July 2014.
7. Trentini, G. V., "Partially reflecting sheet arrays," *IEEE Trans. Antennas Propag.*, 666–671, 1956.
8. Chen, X. D., T. M. Grzegorzczuk, B. Wu, J. Pacheco, Jr., and J. A. Kong, "Rebuts method to retrieve constitutive effective parameters of metamaterials," *Physical Review E*, Vol. 70, 016608, 2004.